Detection of sunken defects on the FPC trace

LI Dejian, YUAN Weiqi

(*Computer Vision Group*, *Shenyang University of Technology*, *Shenyang* 110870)

Abstract: Trace is the important composition structure of printed circuit board, which connects the devices, it is also the module that taking up the highest proportion, thus, it is the major testing target of quality assurance. The sunken defects proposed in this paper is a width abnormity defect on the FPC trace, which would cause the latent open circuit defect and affect the electrical function of circuit. The problem of flexible deformation and width difference make the FPC trace detection harder. Therefore, this paper proposed a detection scheme combined with linear masks and circle distribution characteristic. Firstly, this scheme preprocessed the acquired FPC image, divided the trace into several sub-regions and obtained the line width values of each trace transverse section. Then the line width sequences were searched with the linear difference template of gray scale. Thus, the sunken defects alternative positions were located. Lastly, the circle distribution characteristic is defined to identify the real defect areas from the alternative regions acquired from the previous step. Thus, the detection of sunken defects on the FPC trace was accomplished. The algorithm was tested in the self-built image database, which shows the better detection performance than the other typical algorithms.

Keywords: FPC; Trace; Sunken Defect; Linear Difference Template; Line Width Sequences; Circle Distribution Characteristic

1 Introduction

Flexible printed circuit board (FPC) is a special kind of printed circuit board (PCB), which is widely used in various electronic products with the advantages of free bend and gauzy quality. Among these, the FPC composes of the base material of polyester film and the conductive material of silver paste, which is with the advantages of low price, high dimensional accuracy and low moisture absorption ratio[1-2]. During the production process, the jam of mesh holes leads to the sunken defects on the FPC trace, which affects the whole performance of circuit board. Therefore, it is necessary to find the defective boards for later reprocessing or rejecting. The traditional detection method of sunken defects on the FPC trace is eyes observation, which is ineffective, imprecise and inadequate for the requirements of modern automation production line. At present, the automated detection methods mainly include electrical testing, Automatic Optic Inspection (AOI) and Automatic X-ray Inspection (AXI)[3-4]. Currently, AOI turns into the mainstream research direction of PCB (including FPC) detection with the advantage of non-contact, simple structure and high repeatability.

From the point of principle, the AOI methods of sunken defect detection could be divided into reference contrast method[5-12] and rule evaluation method[13]. The core concept of reference contrast method is the contrast between measuring board and standard board, which could be further divided into image contrast, characteristic contrast and line width contrast. This method is effectively aiming at the typical deformation-free FPC image. But as FPC can deform arbitrarily, the images are usually transformative with various degree in the acquirement process. It presents as the curve and transposition of trace and would seriously impact the detection performance of this method. These three methods are: (1) image contrast: This method firstly matches the measuring image with standard image, contrasts the difference and thereby detects the defect. While because of the bad matching performance which aroused by the deformation, the detection accuracy rate is rather low[8-9]. (2) characteristic contrast: Certain characteristic would be compared, which extracted from measuring board and standard board. Such as literature[10], it detects the defect through comparing density distribution of image edge. In the literature[11], the gradation histogram is compared, analogously, the literature[12] compares area for detection. Due to the existence of flexible deformation, the image is stretched or compressed locally and wholly, which affects the characteristics such as form and area of the trace and further deduces the detection accuracy. (3) line width contrast: This method firstly acquires the width values of trace, and then compares with standard width value. However, there are more than one standard width values in the whole FPC and acquirement of the theoretical line width still needs methods such as template matching, which also affected by the flexible deformation. In terms of rule evaluation method, it judges the trace whether there is a defect or not through the defined rules. However, the researches on this method are scarce, mainly including literature[13], which is based on trace edge linear fitting. It detects the sunken defects via the difference between the real edge and fitting line of the trace, but flexible deformation makes the straight line curving. Thus the poor fitting performance reduces the detection performance.

Inbrief, there is not a method that could effectively detect sunken defects on the FPC trace on the condition of flexible deformation and inconsistent line width. Hence, this paper proposes a detection scheme based on linear difference template and line width sequences searching. This method acquires trace width information, which is stored in sequences. The defects are detected via the distribution characteristic of sequence and the defined circle distribution characteristic. It could deal with the problem of flexible deformation and there is no need to acquire standard line width value beforehand.

2 Feature analysis

2.1 Feature analysis of FPC trace

The FPC image consists of background and circuit, and the circuit includes trace and non-trace, such as bonding pad, LED pedestal and so on. Fig.1 is a local screenshot from acquired FPC image, it can be seen that the black region is background, the white area is circuit, the parts in the gray frame are non-trace regions and the other parts are trace regions. As it is shown, the trace could possess three basic forms, such as 'straight line', 'bending line' and 'crossed line'. Meanwhile, there are several sizes of line width in a FPC image and even a strip of trace has different sizes, it is shown as the red rectangular frame in Fig.1.

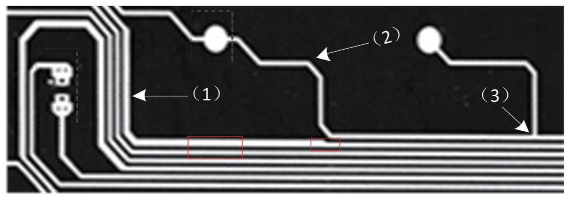

Fig. 1 Local screenshot of FPC image

2.2 Feature analysis of sunken defect

Sunken defect may occur on any position of the trace with the various depth D and Length L, as shown in Fig.2(a). Fig.2(b) is the distribution curve of trace transverse section line width value in Fig.2(a). As is shown, the trace line width on sunken defect position is smaller compared with its both sides, which could be the distribution characteristic for detection.

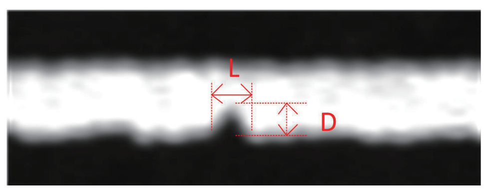

(a) Sunken defect

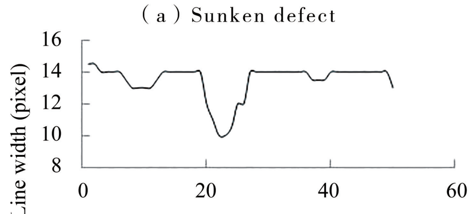

(b) Distribution curve of line width

Fig. 2 Sunken defect and distribution curve of line width

As shown in Fig.3, there are normal bending line traces where distribution curve of line width is similar to sunken defect, because the segment cd is indeed narrower relative to segment ac and db, it is important to distinguish them. Through observation, in Fig.2(a) and Fig.2(b), the change of width value always occurs on the positions of bend, so it could be identified from the real defects.

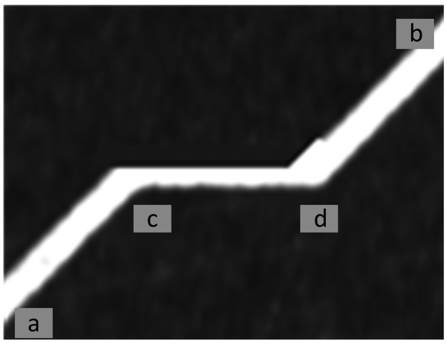

(a) Bending line trace with narrow interlude

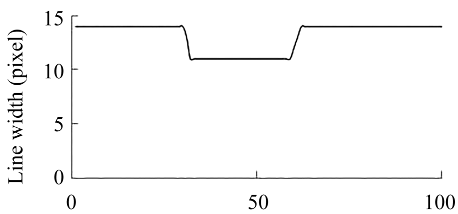

(b) Distribution curve of line width

Fig. 3 Certain bending line distribution curve of line width

3 Defect detection

3.1 Preprocess of the FPC image

Preprocess of the FPC image isto locate the region of interest (ROI), which is trace region. According to above analysis, a FPC image consists of bonding pad, LED pedestal, trace region and so on. The shape and size of these non-trace regions are basic constant. Hence, against image I_{ori}, the templates of non-trace regions are established via the literature[14] method. Then the non-trace regions R_{other} are located using the template matching methods in literature[15], and I_{pre} is acquired through the process of formula (1). At last, the trace region R_{real} is extracted via the OTSU method in literature[16].

$$I_{pre}(i,j) = \begin{cases} B, (i,j) \in R_{other} \\ i_{ori}(i,j), (i,j) \notin R_{other} \end{cases} \tag{1}$$

In formula (1), B is a constant which represents the gray average of FPC background, which is confirmed as 17 through observation and statistics.

3.2 Extraction of alternative regions based on linear difference template

The generation of trace width sequence needs three steps, the detailed description is as follows.

1) Acquiring line width of trace sections. Firstly, in terms of the trace regions R_{real}, the distance between pixels is calculated through the distance transformation algorithm in literature[17]. Then through the method of literature[18], the 'pure' skeleton S_{nai} is acquired after gaining the skeleton of R_{real} and pruning branch noise using the method of literature[18]. The distance value of the pixels on S_{nai} could be regarded as the width value of R_{real} transverse section.

2) Dividing the trace into sub-regions. The points on S_{nai} would be removed if they satisfy the formula (2), then the S_{nai} is divided into skeleton segments Si, and the variable i is index, which ranges from 1 to n. The corresponding trace region of each segment Si is a sub-region of trace R_i. In the formula (3) and (4), the variable u and v are associated with variable j and i respectively, their values depend on j, i and the incidence relation defined in the formula.

$$C_{col} + C_{row} = 6 \tag{2}$$

$$C_{col} = \sum_{u=j-1}^{j+1} [abs(g(i-1,u) - g(i,u)) + abs(g(i,u) - g(i+1,u))] \tag{3}$$

$$C_{row} = \sum_{v=j-1}^{i+1} [abs(g(v,j-1) - g(v,j)) + abs(g(v,j) - g(v,j+1))] \tag{4}$$

3) Generating the sequence of trace width. Regarding to a endpoint of Si as starting point, it is traversed in the order of skeleton tracking[19]. In the traversal process, the line width distance value w (p_i) of relevant position p_i is acquired point-by-point, thus, the line width sequence of the sub skel-

eton region is generated. Such as the sub trace region in Fig.4(a), the white region is trace, the black region is background, the grey dotted line $p_l p_r$ is the trace skeleton S_i, and p_l and p_r is its left endpoint and right endpoint. And the Fig. 4 (b) is the line width sequence generated from the point p_l which is marked using grey arrow.

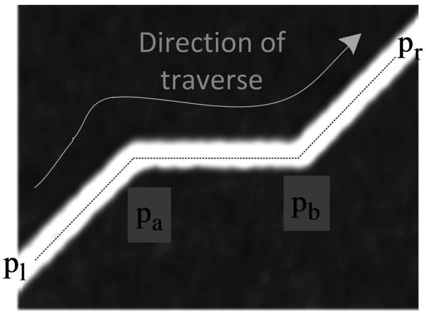

(a) Certain sub region of trace

W(pl)		...		W(pi)		...		W(pr)

pl ... pi ... pr

(b) Line width sequence of trace region

Fig. 4 Certain sub trace region and line width sequence

Through the observation towards the sunken defects in the FPC image base, the width range of sunken defects along the trace trend is less than 90 pixels. Thus, an one-dimensional linear difference template with the length L 91 is defined for extracting the whole sunken defect regions. When the index $w(p_i)$ of certain position p_i inside the template differs with the index of template's both ends, the present position p_i is regarded as abnormal position if the difference value is larger than threshold, a specific definition is shown as formula(5). Then the index of abnormal position is stored in set Q, and the corresponding mapping position on the trace is defective region.

$$w(p_1) - w(p_{\frac{r-1}{2}}) > k$$
$$\text{AND} \quad w(p_r) - w(p_{\frac{r-1}{2}}) > k \qquad (5)$$

In formula(5), $w(p_i)$ is the sequence value of position p_i in template, l=1 means the left endpoint of template and r=90 means the right endpoint of template. The threshold k is the normal floating range of trace width, and it could be acquired as follows. In the image base, the trace segments R_j are picked up (j is the index of trace and it ranges from 1 to n.), the amount is n. The line width distribution range of each trace segment is stated, which is noted as $\min[w(R_j)] \sim \max[w(R_j)]$. The line width volatility deviation of trace segment R_j is $e(j) = \max[w(R_j)] - \min[w(R_j)]$ and the evaluation of k is shown as formula(6).

$$k = \max_{j=1,2,\ldots,n} e(j) \qquad (6)$$

Aftertraversing the whole width sequence with the template, the p_i of each position in sequence is binary, shown as formula(7). If $p_i \in Q$, it is regarded as the goal; otherwise, it is the background. Thus, the binary sequence $t(i)$ is acquired.

$$t(i) = \begin{cases} 1, p_i \in Q \\ 0, p_i \notin Q \end{cases} \qquad (7)$$

The Fig. 5 is the extraction effect sketch map. A_j is the corresponding line width sequence of trace segment R_j. When the condition is $d<L$, the whole object region is extracted completely, shown as Fig. 5 (a) & (b). When the condition is $d \geq L$, there is not any region to be extracted, which makes the situation in Fig.5(c) eliminated. So after the template searching, all of the defective regions and some blending regions are extracted, but the way to distinguish them needs to be considered.

3.3 Recognition of sunken defect based on circle distribution characteristic

As there are different line width values for different trace segments, the non-defective regions that length d is shorter than liner template length L would also be extracted , shown as Fig.5(b).

So this paper puts forward a method based on circle distributioncharacteristic to detect the real defect.

As shown in Fig.6, L_{ine} is a curve and the circle C_{ir} is established with the radius R and center O, which may be any point in L_{ine}. And there are two crossing points of curve L_{ine} and circle C_{ir}, which are

P_1 and P_2. Then the circle C_{ir} is divide into two parts: C_1 and C_2. The circle distribution characteristic V on the position O is defined as formula (8).

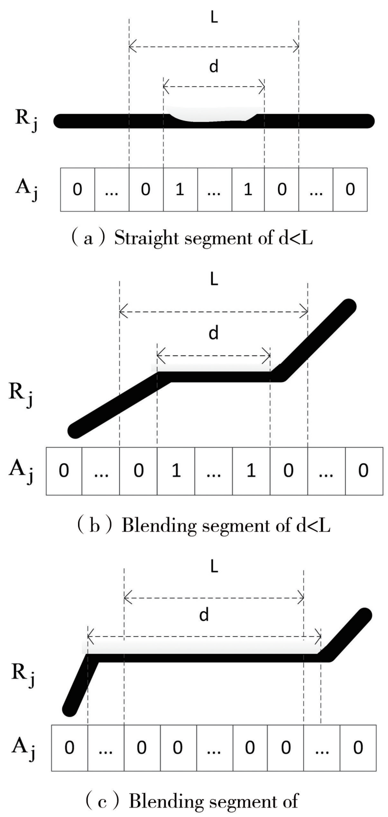

(a) Straight segment of d<L

(b) Blending segment of d<L

(c) Blending segment of

Fig. 5 Relationship of d、L and detection result

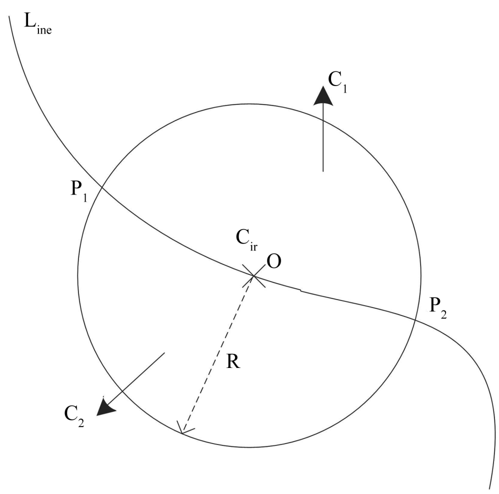

Fig. 6 Definition of circle distribution characteristic

$$V = \frac{min[\Phi(c_1), \Phi(c_2)]}{max[\Phi(c_1), \Phi(c_2)]} \quad (8)$$

$\Phi(*)$ means the area of region '*'.

Firstly, the extracted defect regions are labeled on sequence, then the sub-regions $f_s(j)$ are generated. j is the index of regions, which ranges from 1 to m. The form of sub regions appears as segment which is long or short. Then the left endpoint and right endpoint are gained, denoted as p_{le} and p_{ri}. The two endpoints of each connected domain are mapped to relevant skeleton of FPC trace, denoted as s_{le} and s_{ri}. According to the method of chapter 3.3, the relevant characteristic variable is gained with circle center (s_{le}, s_{ri}) and radius R. relevant skeletons serve as segmentation curves, which are denoted as V_1 and V_2 respectively. At last, the region $f_s(j)$ is estimated via formula(9).

$$\begin{cases} V_1 > T \quad \text{AND} \quad V_2 > T, Ture \\ V_1 \leqslant T \quad \text{OR} \quad V_2 \leqslant T, False \end{cases} \quad (9)$$

In formula(9), 'True' means that the region R_s between s_{le} and s_{ri} belongs to defect, 'False' means that R_s is not a defect. T is a threshold that the value is determined through the experiment. The condition $V \leqslant T$ means the point locates the turning place of trace; otherwise, it locates the non-turning place.

4 Experiment design and result analysis

4.1 Image base establishment

The image base named SUT-F3 is established for the verification of algorithm. The image is acquired from production line which manufactures FPC of laptop keyboard, and the size is 7500 * 8192. The adoptive industrial camera is P4-CM-08K070 line-scan digital camera from DALSA, and the light source is OPT-LST562-W from OPT. The acquisition is with the help of lead screw and grating ruler. The image base contains 51 images, with 257 sunken defects among them. Fig.7 is the image acquisition device, and the FPC image sample is shown as Fig.8.

4.2 Definition of evaluation indicator

To evaluate the algorithm performance quantitatively, false recognition rate(FRR) and false detection rate(FDR) are defined, shown as formula (10) and (11):

$$FRR = \frac{NLD}{NAD} \times 100\% \tag{10}$$

$$FDR = \frac{NND}{NAE} \times 100\% \tag{11}$$

In the formula, NLD is the number of loss defects, NAD is the number of all defects, NND is the number of non-defects and NAE is the number of all segments.

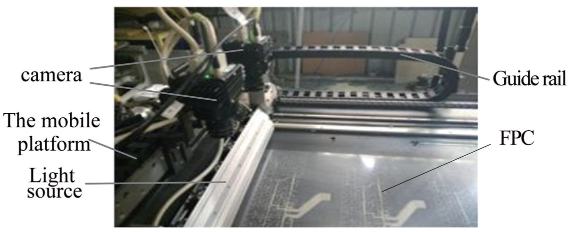

Fig. 7 Image acquisition device

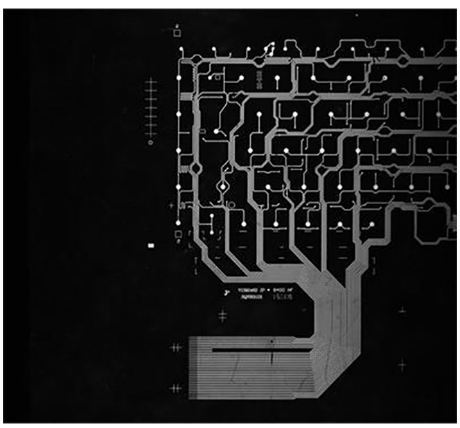

Fig. 8 Sample in FPC image base

To evaluate the algorithm performance of chapter 3.3 on judging whether the endpoint is in blending region or not, the rate of point error recognition (REC) and rate of points error rejection (REJ) are defined, shown as formula (12) and (13):

$$REC = \frac{NFA}{NAT} \times 100\% \tag{12}$$

$$REJ = \frac{NFR}{NANT} \times 100\% \tag{13}$$

In the formula, NFA is the number of false accept, NAT is the number of all turning points, NFR is the number of false rejection and NANT is the number of all non-turning points.

The equal error rate (EER) is usually used to evaluate the integrated recognition performance of a system. The acquirement method is getting the curve crossing point of FDR and FRR (REC and REJ) on the same condition. The less EER means the better system performance[20].

4.3 Experiment result analysis

Ten images are selected from the image base randomly, and 63 defect regions are acquired after processing via the algorithm of chapter 3.3. The total number of 126 acquired endpoints are mapped to the skeleton of origin image, there are 48 endpoints lying on the blending regions and 78 on the non-blending regions. Through the statistics of trace line width W, it ranges from 13 pixels to 20 pixels. Hence, the circle distribution characteristic parameter R is confirmed as 20, then the judging ability of the endpoint position on the trace could be acquired when V from 0 to 1. Shown as Fig.9, when V is equal to 0.9, REC = REJ = 0.085, which means EER is equal to the minimum value 8.5% and the detection system achieves the best performance. Thus, T is confirmed as 0.9 ultimately.

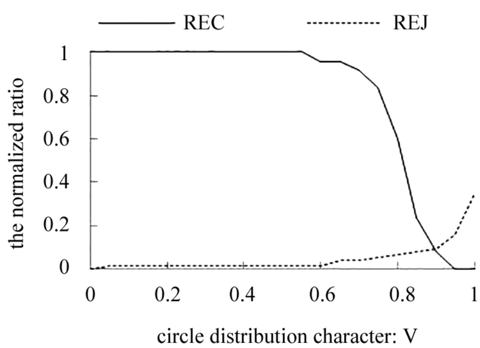

Fig. 9 Determination of constraint set parameter

To compare the sunken defects detection performances of the method in this paper and other methods, 51 images in the image base SUT-F3 are tested, the result is shown in Table 1.

It can be seen from Table 1 that linear difference template method is as low as 8.71%, which reduces at least 4.94% compared to other methods, it reveals the practical application value of this method on sunken defects on FPC trace. From a comprehensive perspective, the reasons why this method could achieve an excellent performance are the robustness to flexible deformation and the independence on standard line width value.

Table 1 Experiment results

Method	EER(%)
Gray contrast[9]	29.72
Area contrast[12]	28.35
Line width contrast[13]	17.02
Gray histogram contrast[11]	16.98
Edge density contrast[10]	13.65
Linear difference template	8.71

5 Conclusion

The detection of trace sunken defect is an important part in FPC mass detection. To solve the problem of flexible deformation and various line width, this paper puts forward a solution based on liner difference template and circle distribution characteristic after particular feature analysis. The algorithm principle and identification process are expounded in detail, so do the evaluation indicator and parameter setting method. The algorithm was tested in the self-built image database. The results show that the EER of contamination defects detection method proposed in this paper is only 8.71%, which decreases 4.94% at the last comparison to the other typical algorithms EER. It indicates the superiority and practical application value of the method proposed in this paper.

For the betterperformance in the practical detection application, the cases of missing and false inspection would be analyzed further.

References

[1] Ruchir V N. (2016). Bare PCB Verification System Using Optical Inspection & Image Processing. *International Research Journal of Computer Science*, 3(4), pp. 39-50.

[2] Glatzl, T. (2016). Development of an air flow sensor for heating, ventilating, and air conditioning systems based on printed circuit board technology. *Sensors and Actuators A: Physical*, 237, pp. 1-8.

[3] Hyung, T K. (2015). Quick and efficient light control for conventional automatic optical inspection (AOI) systems. *International journal of precision engineering and manufacturing*, 16(2), pp. 247-254.

[4] Sajal, R F. (2008). A machine vision based automatic system for real time recognition and sorting of Bangladeshi bank notes. *International Conference on Computer and Information Technology*, pp.533-535.

[5] Liao, C T. (2012). A flexible PCB inspection system based on statistical learning. *Journal of signal processing systems for signal, image, and video technology*, 67(3), pp. 279-290.

[6] Wang, L. (2016). Calculation of flexible printed circuit boards (FPC) global and local defect detection based on computer vision. *Circuit World*, 42(2).

[7] Zulkoffili, Z. (2015). Template based defect detection of flexible printed circuit. *Jurnal Teknology (Sciences & Engineering)*, 78(1), pp. 153-158.

[8] Luo, L. (2011). Embedded Inspection System for FPC Based on Machine Vision. *Computer Measurement & Control*, 78(1), pp. 153-158.

[9] Li, P. (2015). Research on PCB Industry Line Detection System Based on Machine Vision. *Kunming University of Science and Technology.*

[10] Chen, Z W. (2015). Key image processing technology in optical defect inspection of FPC. *Guangzhou: South china university of technology.*

[11] Kong, L D. (2013). Research on Defect Detection Algorithms and System for Flexible Printed Circuit Board. *China Jiliang University.*

[12] Huang X H. (2012). Research on Key Technologies of AOI System for PCB Inspection. *Nanjing University of Information Science & Technology.*

[13] Qiao, N S. (2013). Circuitry detection in printed circuit board. *Acta Photonica Sinica*, 42(11), pp. 1355-1359.

[14] Zhang, J. (2013). Appearance detection for printed circuit board by Gerber file. *Optics and precision engineering*, 21(10), pp. 2679-2687.

[15] Wu X J. (2013). High performance template matching algorithm based on edge geometric features. *Chinese Journal of Scientific Instrument*, 34(7), pp. 1462-1469.

[16] Otsu, N. (1979). A threshold selection method from

gray-level histograms. *IEEE Transactions on Systems, Man, and Cybernetics*, 9(1), pp. 62-66.

[17] Saito, T. (1994). New algorithms foreuclidean distance transformation of an n – dimensional digitized picture with applications. *Pattern Recognition*, 27(11), pp. 1551-1565.

[18] Yuan, W Q. The circuit break detection of flexible deformation FPC based on skeleton. *Chinese Journal of Scientific Instrument*, 38(4), pp. 996-1004.

[19] Liu, K. (2001). The Study on Automatic Tracking Method of Typhoon Spiral Cloud Bands. *Computer Engineering*, 27(10), pp. 152-154.

[20] Badrinath, G S. (2011). Stockwell transform based palm-print recognition. *Applied Soft Computing*, 11(7), pp. 4267-4281.

Authors' Biographies

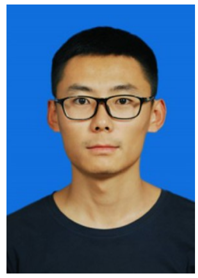

LI Dejian received B.Sc. from Shenyang University of Technology in 2013. Now he is a doctoral candidate in Computer Vision Group, Shenyang University of Technology. His main research field is machine vision and biometric identification.

E-mail: 540785944@qq.com

YUAN Weiqi received B. Sc. degree from Hunan University in 1982, received M. Sc. and Ph. D. degrees both from Northeastern University in 1988 and 1997, respectively. Now he is a professor and doctoral supervisor in Shenyang University of Technology. His research interests include machine vision and biometric identification.

E-mail: yuan60@126.com